COBEM 2023 27TH INTERNATIONAL CONGRESS OF MECHANICAL ENGENEERING

ABCM Brazilian Society of Mechanical Sciences and Engineering
27th ABCM International Congress of Mechanical Engineering
December 04-08, 2023, Florianópolis-SC, Brazil

COBEM2023-2176
DESIGN OF RST DIGITAL CONTROLLER AND PLC IMPLEMENTATION ON A WATER LEVEL BENCH

Marco Antonio dos Santos Caballero
Paulo Roberto Oliveira Martins
Gustavo Cunha da Silva Neto
Federal University of Amazonas / UFAM, Department of Mechanical Engineering, Manaus, Amazonas, Brazil
marco.caballerosc@gmail.com
prmartins@ufam.edu.br
gustavoneto@ufam.edu.br
Florindo Antonio Ayres Júnior
Federal University of Amazonas / UFAM, Department of Electrical Engineering, Manaus, Amazonas, Brazil
florindoayres@ufam.edu.br

Abstract. *This work describes the stages of plant modeling, simulation, control design of RST digital controllers and their implementation based on a programmable logic controller (PLC) for an industrial water tank level control bench. The system presents slow first-order dynamics with time delay, centrifugal pump power saturation, and dead zone until reaching the operating range. The digital controller design was carried out through the pole placement technique for the tuning process requiring settling time reduction, zero steady-state error, and robustness. For implementation, the R, S, and T coefficients were calculated through the Diophantine equation, and the programming was developed using Ladder logic on the software CCW (Connected Components Workbench). Five digital controller strategies using the RST structure were designed, namely: a classical PID, a two degree-of-freedom PID, two types of RST with additional poles and an RST with Model Reference Control. All the controllers were simulated and experimentally tested on the bench. For tracking tests sequential multiple steps were performed in different operating regions and for regulation and robustness evaluation single step tests with plant input and output disturbances were also carried out to proceed with a comparative performance analysis of the different strategies. The integral of time absolute error (ITAE) criterion, settling time and peak overshoot were evaluated. It was observed that the five RST strategies developed in this work met the design requirements satisfactorily, enabling a shorter settling time, zero steady-state error and good robustness performances. The high-order RST controllers and MRC RST presented better results than the PID ones.*

Keywords: *RST, digital control, PLC implementation, level control, pole placement.*

1. INTRODUCTION

Given recent advancements in the industry and the subsequent proliferation of computers and microprocessors within the industrial sector, it is imperative to explore control systems that are more sophisticated and capable of maintaining robustness in the presence of nonlinearities, uncertainties, or disturbances (FERREIRA, 2021).

Rani et al. (2014) emphasizes the significance of process automation, specifically regarding level control, as industries frequently handle liquids throughout various stages of production. Tank systems equipped with valves, for instance, are extensively employed across sectors such as chemical industry, water treatment plants, oil and gas platforms, boiler operations, and numerous other applications. Moreover, depending on the specific application, the volume of liquid involved can range from a few to several thousand liters. Consequently, precise measurement and control of liquid levels are of utmost importance. In light of this requirement, industries are actively seeking more advanced and sophisticated control systems, specifically digital controllers.

According to Landau and Zito (2006), digital control is the most suitable approach for accommodating system variations. The use of logical algorithms in digital control facilitates process changes, offering enhanced flexibility and cost reduction compared to traditional analog controllers.

Gonçalves (2019) states that among digital controllers, the RST structure provides the advantage of possessing two degrees of freedom. The term T stand for a polynomial associated to tracking the reference input, while the terms R and S are other two polynomials concerned with regulating the dynamic response at the system output.

The objective of this study is to implement RST controller strategies directly in the Rockwell Micro820 PLC using Ladder programming language and compare their performance with respect to tracking, regulation, and robustness.

Hence, this article is structured as follows: Section 2: Digital Controllers; Section 3: Pole Placement Method; Section 4: Experimental Water Level Bench Description; Section 5: RST Controllers Strategies; Section 6: Simulation; Section 7: Implementation; Section 8: Results and Discussion; Section 9: Conclusions; Section 10: References.

2. DIGITAL CONTROLLERS

According to Franklin *et al.* (2020), a digital controller operates with discrete signals and is physically implemented as a routine or program to be executed by a microprocessor or microcontroller. Cuenca and Salt (2012) further assert that digital controllers are powerful tools capable of controlling multiple parameters, including liquid level, temperature, pressure, carbon dioxide emission, etc. Additionally, digital controllers offer increased flexibility, compactness, and the ability to process complex algorithms. In the Figure 1, for example, it can observe the canonical structure of an RST Digital Controller (KHETTACHE & ABDESSEMEDB, 2023).

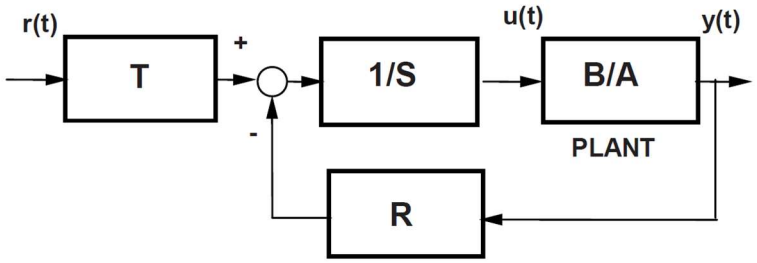

Figure 1. Canonical structure of an RST Digital Controller.

Furthermore, the general control law of an RST digital controller can be expressed as follows (HMAIED *et al.*, 2022; WITRANT *et al.,* 2023):

$$S(q^{-1}) \cdot u(k) = T(q^{-1}) \cdot r(k) - R(q^{-1}) \cdot y(k), \tag{1}$$

where $R(q^{-1})$, $S(q^{-1})$, and $T(q^{-1})$ are polynomials of the form:

$$R(q^{-1}) = r_0 + r_1 q^{-1} + r_2 q^{-2} + \cdots + r_{n_R} q^{-n_R}, \tag{2}$$

$$S(q) = 1 + \ s_1 q^{-1} + s_2 q^{-2} + \cdots + s_{n_S} q^{-n_S} = 1 + S'(q^{-1}), \tag{3}$$

$$T(q^{-1}) = t_0 + t_1 q^{-1} + t_2 q^{-2} + \cdots + t_{n_T} q^{-n_T}, \tag{4}$$

and u(k) refers to the control signal, r(k) to the reference of input and y(k) to the output response of the system in discrete-time and q^{-1} refers to the shift delay operator, so that, $q^{-1} \cdot u(k) = u(k-1)$. In this article the operator $q^{-1}$is replaced by the complex variable z^{-1} when a frequency approach is needed, since the system is considered with linear time-invariant polynomial parameters.
Based on the canonical structure of a digital controller RST seen in Figure 1, we have that the closed-loop transfer function of a controller digital RST is calculated by:

$$H_{MF} = \frac{B(z^{-1}) \cdot T(z^{-1})}{A(z^{-1}) \cdot S(z^{-1}) + B(z^{-1}) \cdot R(z^{-1})} = \frac{B(z^{-1}) \cdot T(z^{-1})}{P(z^{-1})}, \tag{5}$$

where $B(z^{-1})$ and $A(z^{-1})$ are respectively the numerator and the denominator of the discrete plant model. The desired polynomial, denoted as $P(z^{-1})$, incorporates the design objectives for the dynamic characteristics and determines the poles of the closed-loop transfer function.

3. POLE PLACEMENT METHOD

The method consists of a pole assignment by choosing a polynomial $P(z^{-1})$ with desired dynamic response. This polynomial is used to equate the closed-loop denominator polynomial of the combined plant and controller. If necessary, auxiliary poles may be included to achieve order compatibility or high robustness performance. Then, the $R(z^{-1})$ and $S(z^{-1})$ polynomials of the controller are obtained by a Diophantine equation (CHAVOSHI *et al.,* 2023). Finally, the $T(z^{-1})$ polynomial is selected. Details are presented in this section.

3.1 Choice of polynomial $P(z^{-1})$

According to Landau and Zito (2006), a recommended approach for determining the coefficients of $P(z^{-1})$ involves considering a continuous second-order system and selecting two or more parameters such as peak instant, rise time,

settling time, and maximum overshoot. These parameters are chosen to design the desired dynamic response behavior in the output.

Once the parameters are chosen, they are allocated in a second-order system with a canonical transfer function that can be expressed as follows:

$$G(s) = \frac{\omega_n^2}{s^2+2\xi\omega_n s+\omega_n^2}, \tag{6}$$

where ω_n is the natural frequency in rad/s and ξ is the damping coefficient. Furthermore, following the recommendations of Landau and Zito (2006), the natural frequency ω_n and the damping factor ξ must satisfy the following conditions:

$$0.25 \leq \omega_n\, T_s \leq 1.5; 0.7 \leq \xi \leq 1, \tag{7}$$

where T_s is the sampling period in seconds.

However, since the objective is to design a digital controller, it is necessary to discretize the transfer function of Eq. (6) using a sampling period T_s and the Tustin discretization method. This yields the discrete transfer function $G_d(z^{-1})$ as follows:

$$G_d(z^{-1}) = \frac{N(z^{-1})}{P_d(z^{-1})}, \tag{8}$$

where the denominator $P_d(z^{-1})$ contain the dominant poles of the desired polynomial $P(z^{-1})$.

It is important to note that if the parameters $A(z^{-1})$ and $B(z^{-1})$ of the discrete plant have an order greater than two, the polynomial $P(z^{-1})$ would require an order greater than two. That is, the polynomial $P(z^{-1})$ will require additional auxiliary poles that should have minimal influence on the system to ensure that the control system continues to meet the desired performance standards.

$$P(z^{-1}) = P_d(z^{-1}) \cdot P_{aux}(z^{-1}), \text{ where} \tag{9}$$

$$P_{aux}(z^{-1}) = (1 + \alpha_1 z^{-1})(1 + \alpha_i z^{-1})^{n_{aux}-1}, \text{ for i = 2, 3,…} \tag{10}$$

According to Åström and Wittenmark (2013) auxiliary poles are included in the desired polynomial $P(z^{-1})$ to increase its order and improve the robustness of the digital controller they should be within the unit circle to satisfy stability requirements, possess high damping, and exhibit fast transients.

Furthermore, according to Landau and Zito (2006), a typical choice of auxiliary poles is $\alpha_1 = \alpha_2$ or $\alpha_2 = 0$ and the recommended range of choice between:

$$-0.05 \leq \alpha_1, \alpha_2 \leq -0.5. \tag{11}$$

3.2 Diophantine equation

According to Ogata (1995), from the Diophantine equation it is possible to calculate the coefficients of the $R(z^{-1})$, $S(z^{-1})$, and $T(z^{-1})$ polynomials of the RST digital controller. The structure of the Diophantine equation is as follows (WITRANT *et al.,* 2023):

$$A(z^{-1})S(z^{-1}) + B(z^{-1})R(z^{-1}) = P(z^{-1}). \tag{12}$$

With the coefficients of the polynomial $P(z^{-1})$ already determined according to the desired performance of the control system, the aim is to calculate the coefficients of the $R(z^{-1})$ and $S(z^{-1})$ polynomials that satisfy Eq. (12).

In the design of the RST digital controller, the calculation of the Diophantine equation initially seeks to determine the order of each control parameter. Additionally, during the design of the control parameters, certain fixed components should be assigned to ensure specific characteristics, such as zero steady-state error or disturbance rejection in a specific frequency range. The pre-specified components of $R(z^{-1})$ and $S(z^{-1})$ are represented by $H_R(z^{-1})$ and $H_s(z^{-1})$, respectively. Those modifications must satisfy the equations:

$$R(z^{-1}) = H_R(z^{-1})R^*(z^{-1}), \tag{13}$$

$$S(z^{-1}) = H_S(z^{-1})S^*(z^{-1}), \tag{14}$$

Therefore, to achieve zero steady-state error in the system, an integrating action within the $S(z^{-1})$ polynomial, represented by $H_S(z^{-1}) = (1 - z^{-1})$, which represents the discrete version of an integrator, should be included. On the other hand, no pre-specified $H_R(z^{-1})$ was used in this work.

Thus, according to Landau and Zito (2006), to determine the degrees of the polynomials $R(z^{-1})$, $S(z^{-1})$ and $P(z^{-1})$ while incorporating the fixed components $H_s(z^{-1})$ and $H_R(z^{-1})$ the following relationships can be established:

$$n_P \leq n_A + n_B + n_{H_S} + n_{H_R} + d - 1, \tag{15}$$

$$n_S = n_B + n_{H_R} + d - 1, \tag{16}$$

$$n_R = n_A + n_{H_S} - 1, \tag{17}$$

where n_P, n_S and n_R correspond to the degrees of the polynomials $P(z^{-1})$, $S(z^{-1})$ and $R(z^{-1})$, respectively.

After calculating the coefficients for polynomials $R(z^{-1})$ and $S(z^{-1})$, the definition of polynomial $T(z^{-1})$ is still pending. To determine it, two strategies are considered: the first one in which $T(z^{-1}) = R(z^{-1})$ and the second one in which $T(z^{-1}) = R(1)$, that is, equal to the sum of the coefficients of the polynomial $R(z^{-1})$.

4. EXPERIMENTAL WATER LEVEL BENCH DESCRIPTION

The plant used in this article is the control level bench shown in the P & ID diagram in Figure 2. Water is stored in two reservoirs, a main one and an auxiliary one. When a setpoint (SP) is selected in the PLC, a control signal (SC) is transmitted to the frequency inverter, controlling the rotational speed of the centrifugal pump. Water exits the main reservoir and is pumped to the upper region of the tank. The tank is then filled up to the level selected in the PLC. For the level measurement in the tank, a Siemens ultrasonic sensor, The Probe, is used.

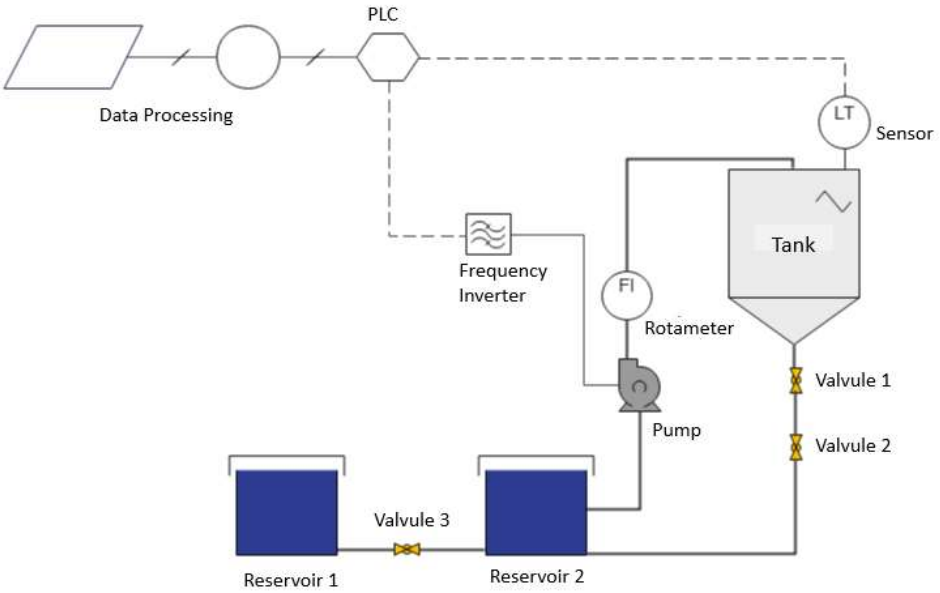

Figure 2. Workbench P & ID diagram.

The pump of the system is a CAM-W10 centrifugal one from DANCOR, with a power of 2 HP, operating on a 220V three-phase power supply and driven by the WEG CFW08 frequency inverter, version 3.95. The maximum working voltage limit of the inverter, for safety reasons, was set to 5V. Therefore, a signal saturation zone which needs to be taken into consideration for the design of digital controllers, as well as an RST structure modification for anti-windup purpose (SILVA ET AL., 2023). The controller used was a Rockwell micro 820 PLC model 2080-LC20-20 QBB, with two expansion modules. Through experimental test, it was verified that the open-loop step response of the plant exhibits a settling time of approximately 1270 s. In the Figure 3 it can be seen the workbench hydraulic circuit and the step response.

The transfer function of the plant model was obtained through the system's open-loop response to a step input and is given by (18)

$$G(s) = \frac{954.15e^{-2s}}{325 \cdot s + 1}, \tag{18}$$

where it represents a first order plant with delay, with a gain of 954.15, time delay of 2 s, and time constant τ = 325s.

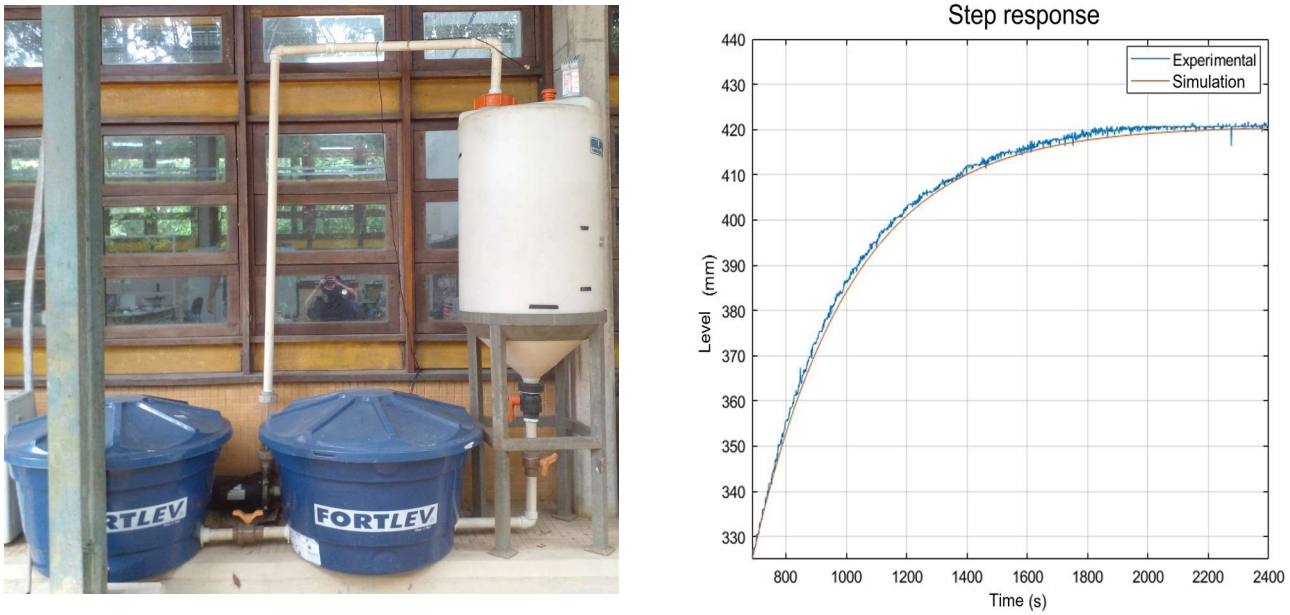

Figure 3. a) Workbench hydraulic circuit on the left side and b) Workbench's step response on the right side.

5. RST CONTROLLERS STRATEGIES

In this article, five strategies of RST digital controllers are designed: the single-degree-of-freedom PID digital controller, denoted as PID 1; the two-degree-of-freedom PID digital controller, denoted as PID 2; RST 1, a classical digital controller of higher order without auxiliary poles; RST 2, which includes two equal auxiliary poles in the control system; and RST 3, which incorporates a first-order reference model with unitary gain and settling time $t_s = 50s$ at the input, along with the inclusion of equal auxiliary poles $\alpha_1 = \alpha_2 = 0.2$ in the control system.

The two main requirements of the project are: 1) to reduce the settling time by approximately 25 times, i.e., around 50 s, and 2) to achieve zero steady-state error. After selecting the project requirements, a sampling period is assigned for discretizing the plant using the ZOH discretization method. Following Nyquist's criteria, where the sampling frequency must be at least twice the maximum operating frequency, and based on criterion showed in Eq. (7), two sampling periods are assigned T_s = 1 is assigned for RST 1, RST 2, and RST 3 digital controllers, while T_s = 3 is assigned for PID digital controllers due to the limitation of this structure to handle systems of higher order than two.

With the transfer function in Eq. (18) already discretized for the adopted sampling periods, calculation of Eq. (6) is performed based on the desired control parameters for the system's dynamic output response, specifically a settling time of 50 s and a maximum overshoot of 2%. Since the desired function P(s) is in the continuous Laplace domain, the aim is to discretize this function in order to obtain the transfer function in (6) and, consequently, the desired polynomial $P(z^{-1})$ for each RST strategy applied in this article.

Finally, for the calculation of $T(z^{-1})$, three distinct situations are considered: for the case of the PID 1 digital controller, since it has only one degree of freedom, the polynomial $T(z^{-1})$ is identical to the polynomial $R(z^{-1})$; in turn, for the PID 2, RST 1, and RST 2 digital controllers, the calculation of the polynomial $T(z^{-1})$ is taken as the sum of the coefficients of the polynomial $R(z^{-1})$, such that $T(z^{-1}) = R(1)$; and the last case, for the RST 3 digital controller, due to the presence of a first-order reference model and, therefore, different dynamics between the controller itself and the reference model, the polynomial $T(z^{-1})$ is calculated as:

$$T(z^{-1}) = vP(z^{-1}), \tag{19}$$

where v is a constant gain calculated as the inverse of the polynomial $B(z^{-1})$.

6. SIMULATION

The simulation of RST digital controllers is performed using the block diagram in Simulink software. The difference between the diagrams lies in the inclusion of the reference model block for the RST 3 digital controller, as well as the inclusion of the anti-windup control tool proposed by Gharsallaoui et al. (2009), where the polynomial S changes position. Instead of being in the direct branch as seen in Figure 1 of this article, the polynomial S is relocated to a feedforward branch along with a delay operator z^{-1} and a constant term equal to 1 in the direct branch. This strategy is implemented

because there is a saturation zone in the voltage that the frequency inverter imposes on the centrifugal pump for safety reasons. This saturation zone ranges from 0V to 5V. The structure with the anti-windup is observed in the Figure 4.

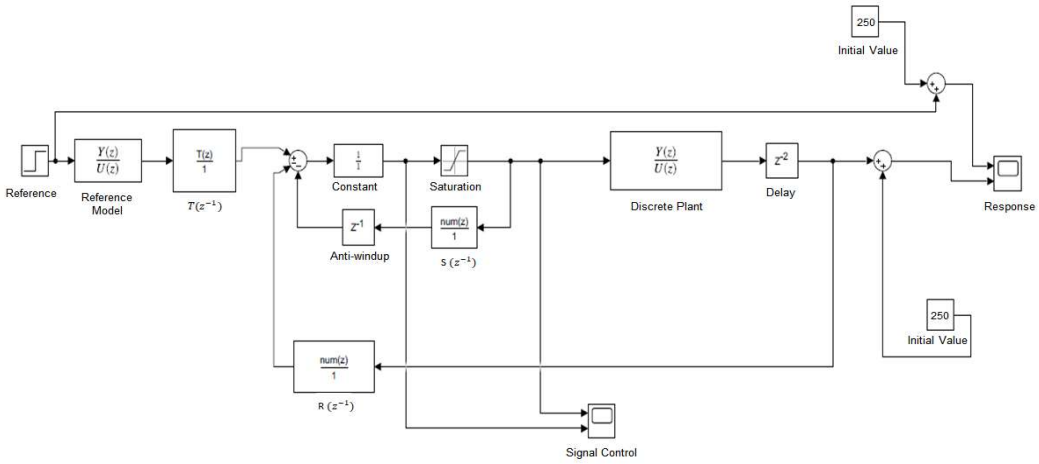

Figure 4. Anti-windup structure.

7. IMPLEMENTATION

The implementation process of the digital controllers in this work consists of two steps: 1) Development of a program in Ladder programming language, which is a logical structure that executes the difference equation of the digital controllers, and 2) Implementation of the discrete-time control laws of the digital controllers, followed by conducting tracking, regulation, and robustness tests while recording the results using the PLC.

Therefore, with the inclusion of the anti-windup method in the digital RST control and simplifying the block diagram during the simulation step, we have:

$$w(k) = T(z^{-1})r(k) - R(z^{-1})y(k) - S'(z^{-1})z^{-1}u(k), \tag{20}$$

where the term $S'(z^{-1})$ refers to the coefficients of the polynomial S, except for the constant $s_0 = 1$, and the term $w(k)$ is related to a new variable that contains the difference equation of the digital controller with the inclusion of the anti-windup method. From these control laws, the difference equations of the RST digital controller strategies are derived at sample instants k, in order to structure a ladder language control algorithm.

The implementation of the sampled difference equations of the RST digital controllers was performed on a PLC using CCW (Connected Components Workbench) software, version 12.0. In this software for the implementation of the program in Ladder language, several logical blocks were utilized, such as timers, FFL and FFU memory stack for storage and unloading, respectively, as well as scale converters and arithmetic blocks, as shown in Figure 5.

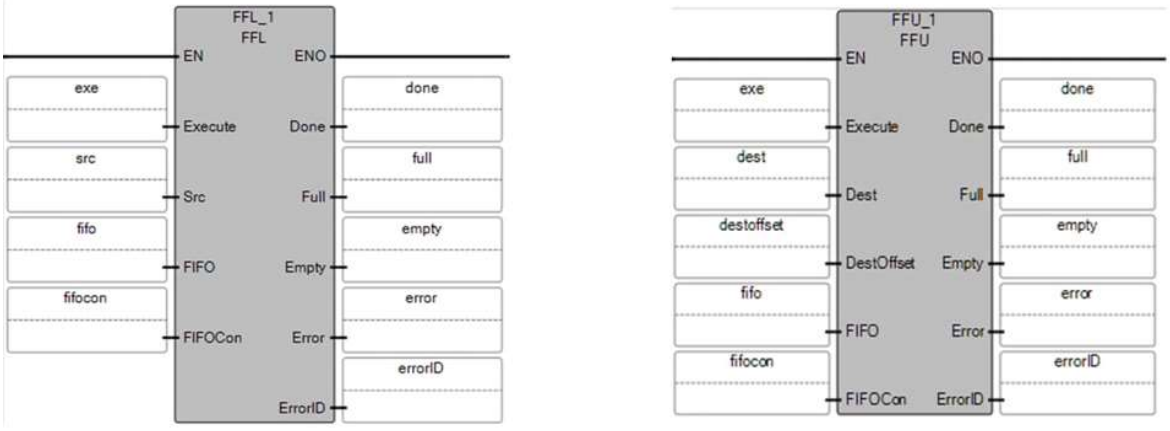

Figure 5. FIFO memory stack. On the left side, we have the FFL loading stack, and on the right side, we have the FFU unloading stack.

8. RESULTS AND DISCUSSION

The coefficients of the polynomials $R(z^{-1})$, $S(z^{-1})$, and $T(z^{-1})$ for each RST digital controller strategy designed in this work can be observed in Table 1.

Table 1. Parameters of the RST digital controllers

PARAMETERS	PID 1	PID 2	RST 1	RST 2	RST 3
r_0	0.056	0.053	0.050	0.039	0.086
r_1	-0.048	-0.048	-0.056	-0.037	-0.078
s_1	-0.718	-0.718	-0.845	-1.245	-1.093
s_2	-0.282	-0.282	0.009	0.387	0.352
s_3	-	-	-0.164	-0.142	-0.259
t_0	0.056	0.008	0.003	0.002	0.341
t_1	-0.048	-	-	-	-0.713
t_2	-	-	-	-	0.492
t_3	-	-	-	-	-0.122
t_4	-	-	-	-	0.009

8.1 Simulation

The simulation was performed using the blocks diagrams in the Simulink software. It is important to note that the sensor's working range corresponds to the cylindrical part of the tank of the Figure 3, disregarding the variable area section. In both simulations and experiments, a step input of 250 mm was initially applied, and the system was allowed to settle at that level. For the simulation of the RST digital controllers, following the aforementioned procedure, a step input of 50 mm was applied in the range of 350 mm to 400 mm over a time interval of 180s to allow for response stabilization. This simulation can be viewed in the Figure 6.

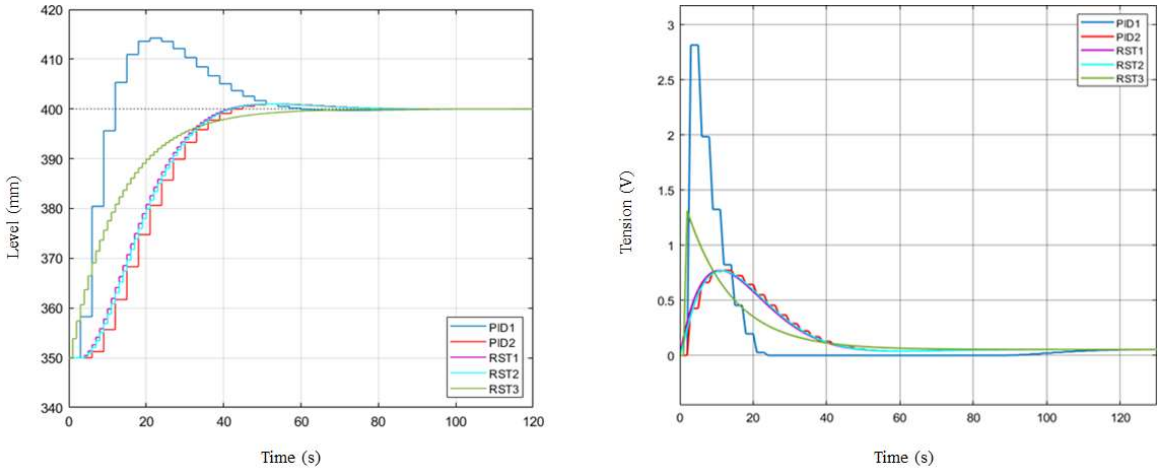

Figure 6. Simulation of the RST Digital Controllers. On the left, we have the response of the controllers to the 50 mm step input, and on the right, the control signal for the 50 mm step input of the RST digital controllers.

From Figure 6, it can be observed that the digital controllers PID2 and RST2 exhibited superior performance in terms of settling time. It is worth noting the RST3 controller, which showed no overshoot. In summary, all digital controllers demonstrated satisfactory results in relation to the design requirements, with the exception of PID1.

8.2 Experiment

By implementing the coefficients of each RST digital controller strategy into the PLC, three experiments were conducted: reference tracking test (multi-step) and two disturbance tests (one at the plant input and another at the plant output).

8.3 Reference Tracking Test

To evaluate the tracking capability of the digital controllers, step tests were conducted for both upward and downward tank level movements. Starting from a water level reference of 250 mm, nine upward steps of 50 mm and eight downward steps of 50 mm were applied. Each test was conducted over a duration of 180 s to ensure stabilization before the next step. The result of this experiment is presented in Figure 7.

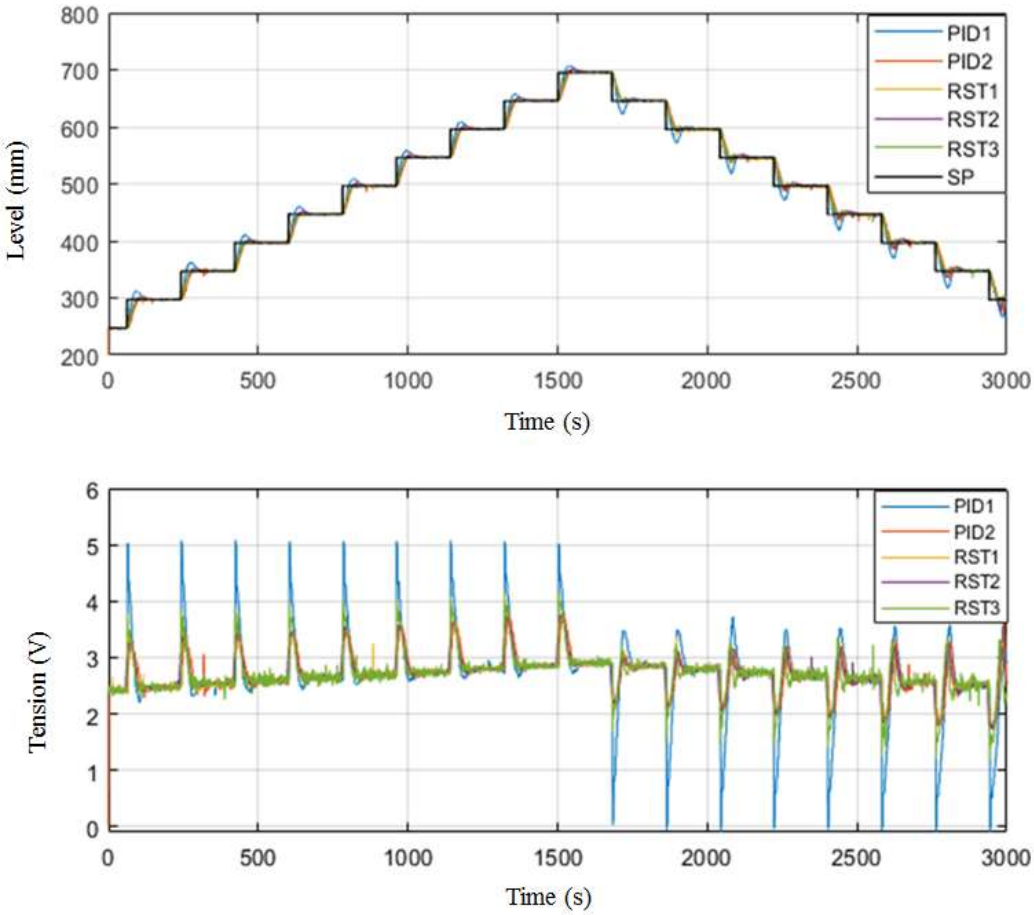

Figure 7. Reference Tracking Multi Step Test. At the top, we have the response of the RST digital controllers to the 50 mm step input, and at the bottom, we have the control signal of the RST digital controllers.

From Figure 7, several performance parameters were calculated, such as settling time t_s, overshoot, signal control's root mean square (RMS), as well as the integral time absolute error (ITAE) and integral time absolute control effort (ITACE) criteria, similarly to the criteria used by Patil *et al.,* 2023, in the water level region of 350 mm to 400 mm, for comparison with the simulations performed on the RST digital controllers. These results can be observed in Table 2.

Table 2. Performance metrics from the multi-step test of the response of the RST digital controllers to the step input in the range of 350 mm to 400 mm.

RST Digital Controllers	t_s (s)	Overshoot (%)	ITAE	ITACE	RMS (V)
PID 1	57.92	25.09	$4.32.10^6$	$2.5.10^6$	2.781
PID 2	64.91	5.92	$4.99.10^6$	$2.47.10^6$	2.715
RST 1	59.95	8.06	$4.79.10^6$	$2.45.10^6$	2.716
RST 2	60.74	9.16	$4.97.10^6$	$2.44.10^6$	2.714
RST 3	40.16	0	$3.57.10^6$	$2.47.10^6$	2.720

Upon examining Table 2 regarding settling time, the RST 3 and PID 1 controllers exhibited the lowest values. Notably, RST 3 showed no overshoot, while PID 2 had an overshoot of only 5.92%. In terms of the ITAE metric, RST 3 had the lowest error, although it consumed the most energy to achieve that.

8.4 Disturbance Tests

To assess the regulation capability and robustness of the digital controllers, simulations of disturbances in the control system were performed. To simulate a disturbance in the plant output, specifically a change in the measured value obtained by the sensor at a specific instant, a 10 mm downward step was configured in the PLC. This disturbance was programmed to occur at 710 seconds when the level was at 400 mm. In turn, to simulate a disturbance in the plant input, a -0.5V step was programmed in the PLC to simulate a potential energy variation in the actuator. This change in the control signal of the system was programmed to occur at 810 seconds when the plant level was at 400 mm. The results of these tests can be observed in Figure 8 and in Tables 3 and 4, which provide performance values evaluated both at the plant output in the interval of 700 to 760 s and at the plant input in the interval of 800 to 870 s.

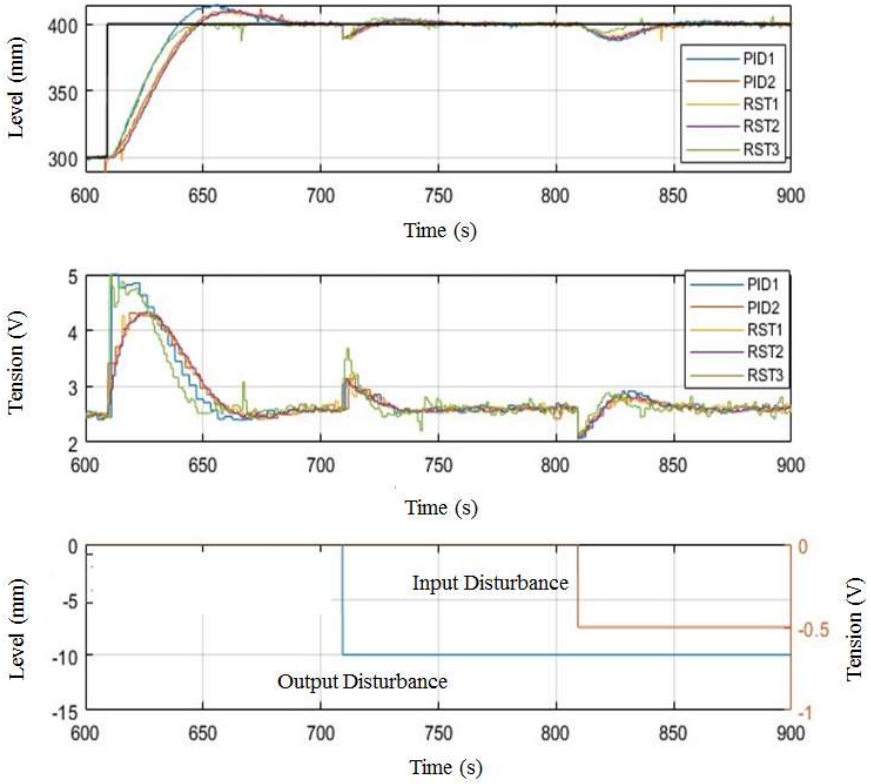

Figure 8. Tests of system output regulation and controller robustness were conducted by simulating disturbances in the system. The top section presents the step response, the middle section shows the control signal, and the bottom section displays the application of disturbances.

Table 3. Performance metrics from the disturbance test at the plant input of the control system.

RST Digital Controllers	t_s (s)	ITAE	ITACE	RMS (V)
PID 1	51.62	$2.42.10^6$	$1.54.10^6$	1.6238
PID 2	49.95	$2.13.10^6$	$1.53.10^6$	1.6234
RST 1	47.12	$1.92.10^6$	$1.53.10^6$	1.6158
RST 2	48.64	$2.01.10^6$	$1.54.10^6$	1.6147
RST 3	33.57	$9.32.10^5$	$1.53.10^6$	1.6127

Table 4. Performance metrics from the disturbance test at the plant output of the control system.

RST Digital Controllers	t_s (s)	ITAE	ITACE	RMS (V)
PID 1	56.62	$1.09.10^6$	$1.17.10^6$	1.6345
PID 2	48.72	$1.08.10^6$	$1.17.10^6$	1.6357
RST 1	40.85	$9.09.10^5$	$1.17.10^6$	1.6360
RST 2	45.12	$1.03.10^6$	$1.17.10^6$	1.6355
RST 3	41.63	$9.45.10^5$	$1.18.10^6$	1.6394

9. CONCLUSION

In this work, five strategies of digital RST controllers were designed and implemented on a level bench. A single-degree-of-freedom digital PID, a two-degree-of-freedom digital PID, an RST controller without auxiliary poles, an RST controller with auxiliary poles, and an RST controller with a first-order reference model and auxiliary poles were employed. In simulations, the RST 2 controller exhibited the shortest settling time, while the RST 3 controller achieved zero overshoot. On the other hand, the PID 1 controller performed the worst, displaying a more oscillatory frequency and higher overshoot than anticipated. Regarding experimental tests, in the step tracking test, the RST 3 controller exhibited zero overshoot in all level regions and was the quickest to stabilize the output response. Based on the obtained results, it can be concluded that the digital controllers yielded better results in the rising tests compared to the descending tests. Furthermore, when subjected to disturbances in the control system, either at the input or the output of the plant, the digital RST controllers demonstrated greater robustness due to their higher-order filters compared to the digital PID controllers.

10. REFERENCES

Åström, K. J., & Wittenmark, B. (2013). Computer-controlled systems: theory and design. Courier Corporation.

Chavoshi, H., Salasi, A., Payam, O., & Khaloozadeh, H. (2023). Experimental Comparison of STR and PI Controllers on a Nonlinear Liquid-Level Networked Control System. In *2023 15th International Conference on Electronics, Computers and Artificial Intelligence (ECAI)* (pp. 1-8). IEEE.

Cuenca, A., Salt, J. (2012). "RST controller design for a non-uniform multi-rate control system". Journal of Process Control, v.22, n. 10, p. 1865-1877.

Ferreira, T.L., et al. (2021). "Controlador RST auto-ajustável: análise e estudo de casos". Trabalho de Conclusão de Curso. Federal University of Alagoas (UFAL), Maceió, Brazil.

Franklin, G.F., David, J., Abbas Emami-Naeini, P. (2020). "Feedback Control of Dynamic Systems". 8º ed. Upper Saddle River: Pearson Education Limited.

Gharsallaoui, H., et al. (2009). "Flatness-based control and conventional RST polynomial control of a thermal process". International Journal of Computers, Communications and Control, v.4, n.1, p. 41-56.

Gonçalves, I.D.S., (2019). "Projeto de um controlador RST para o sistema barra e bola". Igor de Souza Gonçalves – TCC – Universidade Federal do Ceará (UFC), Centro de Tecnologia de Engenharia Elétrica, p.53, Fortaleza.

Silva, V. B., Arce, B. R., de Souza Vieira, P. A., Dos Santos, M. F., Neto, A. F. S., & Mercorelli, P. (2023, June). The Use of Anti-Windup Techniques in Didactic Level Systems: An Interesting Application. In 2023 24th International Carpathian Control Conference (ICCC) (pp. 49-53). IEEE.

Hmaied, H., Sami, H., & Faouzi, B. (2022). Real time control of an upper limb orthosis robot for a passive rehabilitation. In *2022 IEEE International Conference on Electrical Sciences and Technologies in Maghreb (CISTEM)* (Vol. 4, pp. 1-6). IEEE.

Khettache, L., & Abdessemedb, R. (2023). A New Speed Control Approach of Linear Induction Motor Based on Robust RST Controller and Model Reference Adaptive System Estimator. International Journal of Engineering, 36(4), 630-639.

Landau, I.D., Zito, G. (2006). "Digital Control Systems: design, identification and implementation – Communications and control engineering". Springer.

Ogata, K. (1995). "Discrete Time Control Systems". 2nd ed. University of Minnesota, USA: Pearson Prentice Hall.

Patil, M. D., Vadirajacharya, K., & Khubalkar, S. W. (2023). Design and tuning of digital fractional-order PID controller for permanent magnet DC motor. IETE Journal of Research, 69(7), 4349-4359.

Rani, L.T. et al., (2014). "Design and implementation of RST controllers for a nonlinear system". IEEE International Conference on Green Computing Communication and Electrical Engineering, ICGCCEE 2014.

Witrant, E., Landau, I. D., & Vaillant, M. P. (2023). A data-driven control methodology applied to throttle valves. *Control Engineering Practice*, *139*, 105634.

11. RESPONSIBILITY NOTICE

The authors are the only responsible for the printed material included in this paper.